Journal of Wind Engineering
and Industrial Aerodynamics 90 (2002) 1435–1452

www.elsevier.com/locate/jweia

Time-frequency analysis of wind effects on structures

A. Kareem*, T. Kijewski[1]

NatHaz Modeling Laboratory, Department of Civil Engineering and Geological Sciences, University of Notre Dame, Fitzpatrick Hall, Room 156, Notre Dame, IN 46556, USA

Abstract

As many physical processes of interest to Civil Engineers manifest nonlinear and nonstationary features, their complete characterization may not be accomplished via Fourier transforms, necessitating a new analysis framework in the time-frequency domain. This paper overviews recent developments in wavelet-based analysis of a number of physical processes of relevance to the Civil Engineering community. It is shown that the dual nature of wavelet transforms, being a simultaneous transform in time and frequency, permits adaptation of a number of traditional system identification and analysis schemes. For example, the extension of wavelet transforms to the estimation of time-varying energy density permits the tracking of evolutionary characteristics in the signal using instantaneous wavelet spectra and the development of measures like wavelet-based coherence to capture intermittent correlated structures in signals. Similarly, system identification methodologies originally referenced in either the time or frequency domain can be extended into the realm of wavelets. Though the application of wavelet transforms in Civil Engineering is in its infancy, as the examples in this study demonstrate, its future shows great promise as a tool to redefine the probabilistic and statistical analysis of wind effects.

Keywords: Wavelet transforms; Coherence; Bicoherence; System identification; Time-frequency analysis; Instantaneous frequency; Instantaneous bandwidth

1. Introduction

Wind-resistant design and construction of buildings and civil infrastructure is becoming critically important in light of the continually increasing losses associated

*Corresponding author. Tel.: +1-219-631-5380; fax: +1-219-631-9236.
E-mail address: kareem@nd.edu (A. Kareem).
[1] Graduate student.

0167-6105/02/$ - see front matter
PII: S0167-6105(02)00263-5

with windstorms worldwide. Accordingly, the significance of risk analysis and the need to surpass traditional deterministic design approaches is of mounting importance for design and construction. Recent developments in probabilistic methods offer a mathematical framework that promises to enable designers to accurately encapsulate statistics of large data sets and model physical phenomenon associated with wind effects on structures. Such models must embrace a probabilistic format in order to characterize the random nature of wind fluctuations in space and time and its interactions with structures. Earlier review articles by the senior author [1–3]: "Wind Effects on Structures: A Probabilistic Viewpoint", "Analysis and Modeling of Wind Effects: Numerical Techniques", and "Modeling and Simulation of Wind Effects: A Reflection on the Past and Outlook for the Future", have focused on the analysis, modeling and simulation of wind-related processes, e.g., pressure fluctuations and structural response.

This paper addresses a topic that goes beyond the customary approach of viewing a random process in terms of either time or frequency by focusing on a time-frequency representation using the wavelet transform. First, a general background of the wavelet transform is presented, followed by discussion of wavelet-based spectral estimates and basic time-frequency insights from wavelet scalograms and coherence and bicoherence estimates in a wavelet framework. This is followed by a discussion of specific system identification approaches exploiting wavelet information in the time domain and instantaneous power spectral analyses rooted in the wavelet frequency domain.

2. Wavelet transform

Commonly used signal processing tools, e.g., Fourier analysis, fail to identify when certain characteristic features occur in a waveform. As Fourier basis functions are localized in frequency but not in time, an alternative was introduced by Gabor to localize the Fourier transform through the short-time Fourier transform (STFT), which provides time and frequency localization [4]. However, constraints of the Heisenberg Uncertainty Principal limit the obtainable resolutions considerably. An alternative approach would be to design basis functions that are also local in both frequency and in time, but capable of adapting their resolutions dependent on the frequency being analyzed, a so-called multi-resolution operator known as the wavelet transform.

The wavelet [5–6] is a linear transform that decomposes an arbitrary signal $x(t)$ via basis functions that are simply dilations and translations of a parent wavelet $g(t)$ through the convolution of the signal and the scaled/shifted parent wavelet:

$$W(a,t) = \frac{1}{\sqrt{a}} \int_{-\infty}^{\infty} x(\tau) g^{*}\left(\frac{t-\tau}{a}\right) \mathrm{d}\tau. \tag{1}$$

Dilation by the scale, a, inversely proportional to frequency, represents the periodic or harmonic nature of the signal. By this approach, time-frequency localization is possible, since the parent wavelet serves as a "window function", as opposed to the trigonometric bases comprised of the sines and cosines of the Fourier transform. The wavelet coefficients, $W(a,t)$, represent a measure of the similitude between the dilated/shifted parent wavelet and the signal at time t and scale (frequency) a.

Though there are countless parent wavelets used in practice, of both discrete and continuous form, the continuous wavelet transform (CWT) using the Morlet wavelet [7] has become quite attractive for harmonic analysis, due to its analogs to the Fourier transform, evidenced by

$$g(t) = \mathrm{e}^{-t^2/2}(\cos(\omega_0 t) + \mathrm{i}\sin(\omega_0 t)). \tag{2}$$

Essentially, the Morlet wavelet in Eq. (2) is a Gaussian-windowed Fourier transform, with sines and cosines oscillating at the central frequency, f_o ($\omega_0 = 2\pi f_0$). Dilations of this temporally localized parent wavelet then allow the "effective frequency" of this sine–cosine pair to change in order to match harmonic components within the signal.

The Morlet wavelet is equivalently localized in the frequency domain, as evidenced by the Fourier transform of the dilated Morlet wavelet in Eq. (2)

$$G(af) = \sqrt{2}\sqrt{\pi}\mathrm{e}^{-2\pi^2(af-f_0)^2} \tag{3}$$

which is utilized in the Fourier-domain implementation of the wavelet transform

$$W(a,t) = \sqrt{a}\int_{-\infty}^{\infty} X(f)G^*(af)\mathrm{e}^{\mathrm{i}2\pi ft}\,\mathrm{d}f. \tag{4}$$

By exploiting the fast algorithms in the Fourier domain, Eq. (4) is often more efficient for implementation. For the Morlet wavelet, there is a unique relationship between the dilation parameter of the transform, a, and the frequency, f, at which the wavelet is focused, allowing the relation of scales to the Fourier frequencies familiar to most engineers. This attractive relationship is evident by maximizing Eq. (3) to yield

$$a = f_0/f. \tag{5}$$

By virtue of the unique relationship between scale and frequency, this wavelet is specifically used later in Figs. 3 and 5–10 in the CWT analyses performed.

Alternatively, a discrete formulation of Eq. (1) may be preferred to minimize the redundant information retained in the continuous transform and provide an orthogonal representation for signal decomposition and reconstruction. By this discrete wavelet transform (DWT), the signal is decomposed into a subset of translated and dilated parent wavelets, evaluated at selected scales and translations corresponding to powers of two. This permits the use of efficient algorithms for estimation of the DWT using a series of high and low pass filters to progressively find the wavelet coefficients from the highest level to the mean value.

2.1. Wavelet analysis potential

Both discrete and continuous wavelets have been applied to a variety of problems ranging from image and acoustic processing to fractal analysis. The ability of wavelets to analyze a wide variety of problems stems from the fact that it provides insights into both the time and frequency domains simultaneously. Thus, in its recent extension to the analysis of stochastic processes of interest to Civil Engineering, wavelets have been adapted to a number of situations where Fourier transforms (for frequency domain analysis) or Hilbert Transforms (for time domain system identification) were traditionally used to define quantities of interest. As shown in Fig. 1, when considering the time and frequency information in tandem, wavelets can be used to determine the times and frequencies at which signal energy content is strongest, through examination of scalograms and coscalograms [8]. More specific insights into the linear and quadratic interplay between two signals in both time and frequency can be gained utilizing wavelet coherence and bicoherence measures [9]. However, by exploiting the dual potential of wavelets, other analysis based primarily in either the time or frequency domain, can also be performed. By tracking the variation of wavelet transform coefficients in the time domain, system identification can be readily performed [10]. Similarly, the distribution of wavelet coefficients with frequency at an instant in time provides a familiar spectral representation whose properties can be monitored with time to provide insights into nonlinear behavior [11]. The subsequent sections will discuss in further detail how each of these analyses are conducted.

2.2. *Wavelets in spectral and correlation analysis*

As discussed in [8], wavelets can be used to estimate the traditional power spectral density (PSD) of a process by disregarding all temporal information. For example, in the discrete case, wavelet coefficients $W_{i,j}$ are used to estimate the PSD by summing the squared coefficients in each octave as shown schematically in Fig. 2. A cospectral estimate between two processes is also possible by replacing the squared coefficient term with the product of the coefficients of each process. The energy captured by this wavelet-based spectral estimation closely matches the actual signal energy, though lacking in frequency resolution. This lack of resolution is alleviated in the case of continuous wavelets, which are not constrained by a dyadic discretization of the frequency domain. However, to truly assess the merits of wavelet-based analysis, the

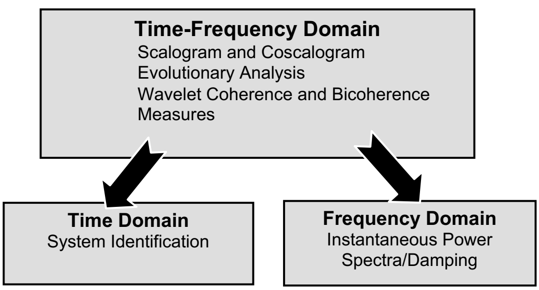

Fig. 1. Potential uses of wavelet transforms for nonlinear and nonstationary signal analysis.

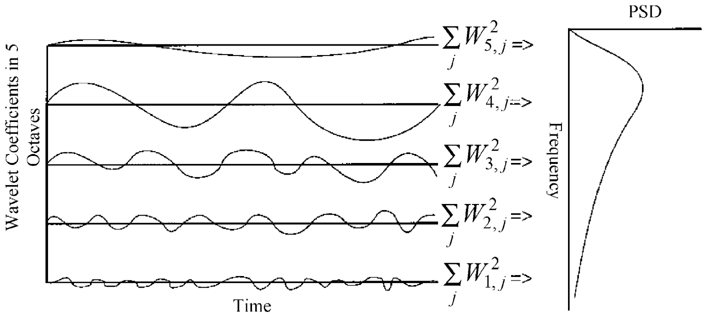

Fig. 2. Summation of discrete wavelet coefficients to estimate power spectrum (after [8]).

valuable temporal information should be retained, prompting the consideration of time-frequency analysis.

2.3. Time-frequency signal representation: scalogram

Similar to the Fourier notion of the power spectrum, an indicator of a signal's time-varying energy content over a range of frequencies can be generated by plotting the squared modulus of the wavelet transform as a simultaneous function of time and frequency to generate a *scalogram* or mean square map. This representation of the localized wavelet transform is well-suited for the analysis of nonstationary phenomena, revealing the frequency content of the signal at each time step to pinpoint the occurrence of transients, while tracking evolutionary phenomena in both time and frequency.

Fig. 3 displays the wavelet scalogram of a sinusoid, whose frequency begins at 0.2 Hz and then decays subtly according to a quadratic function. When viewed in the time-frequency plane, the scalogram largest coefficients, enveloped white, concentrate about a ridge. As discussed in [5], for a particular class of parent wavelet, the ridge scales, or frequencies corresponding to the local maxima of the wavelet transform, provide an estimate of the instantaneous frequency (IF) of the system. Extracting these ridge coordinates provides a pinpoint estimate of the IF of the system, shown in the bottom frame of Fig. 3. The comparison between the actual quadratic IF law of the sinusoid and the extracted wavelet ridge is quite good. Note that the piecewise fit provided by the wavelet can be made more smooth by choosing a finer discretization of scales when evaluating Eq. (1).

In some recent studies, the concept of the scalogram has been advanced to identify correlation between signals in which the squared coefficients are replaced with the product of the wavelet coefficients of two different processes (e.g. [8]). This produces a view of the coincident events between the processes, revealing time-varying pockets of correlation with frequency. Fig. 4 displays such a coscalogram comparison for full-scale pressure measured on a building and the two upstream wind velocity records: the first recorded at the same time as the full-scale pressures under

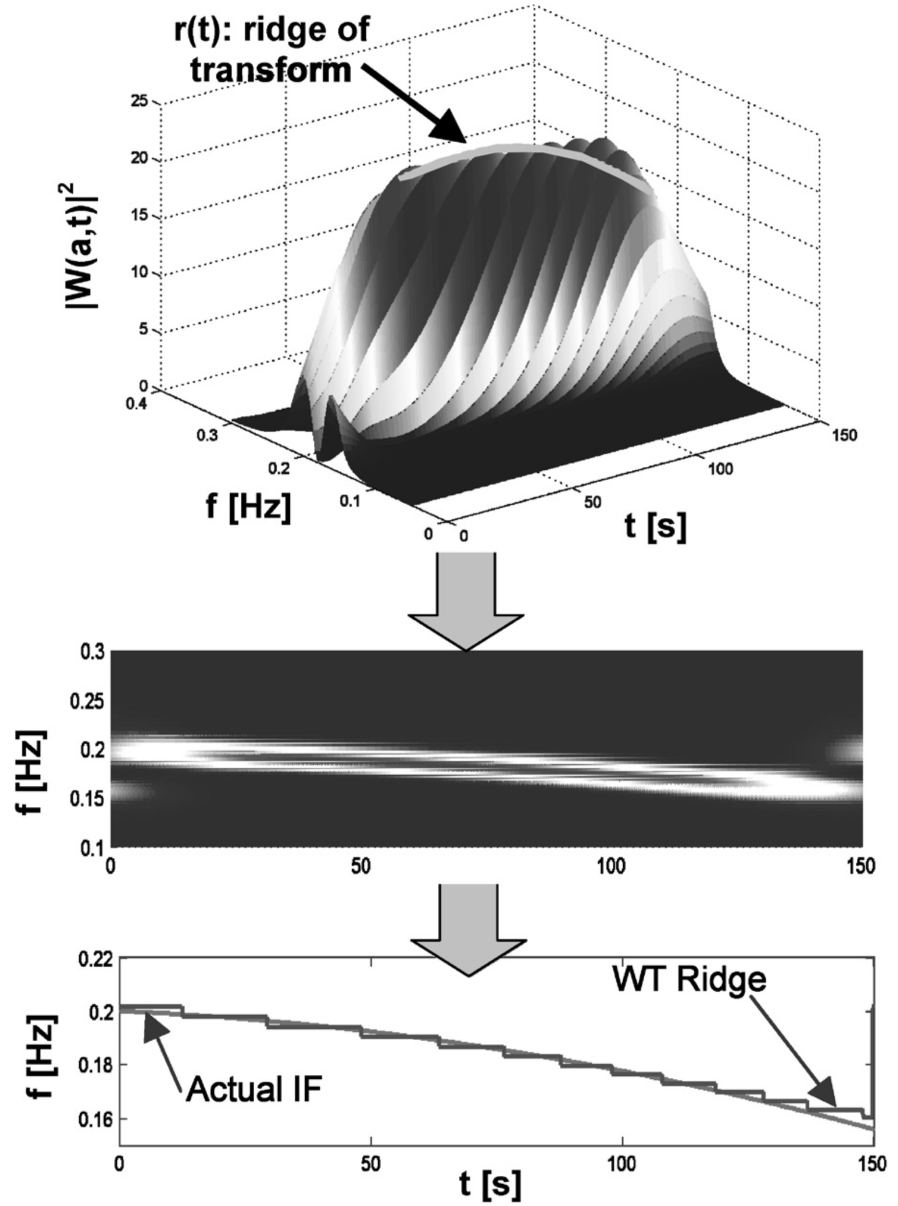

Fig. 3. Wavelet scalogram and extracted ridge for evolutionary signal analysis.

consideration and the second from a different wind event. Fig. 4a–c shows the scalograms and coscalogram of wind pressure and first wind velocity that are knowingly correlated. Note the pockets of white beyond 250 s. This may be compared to a similar analysis for wind pressure and velocity that are known to be

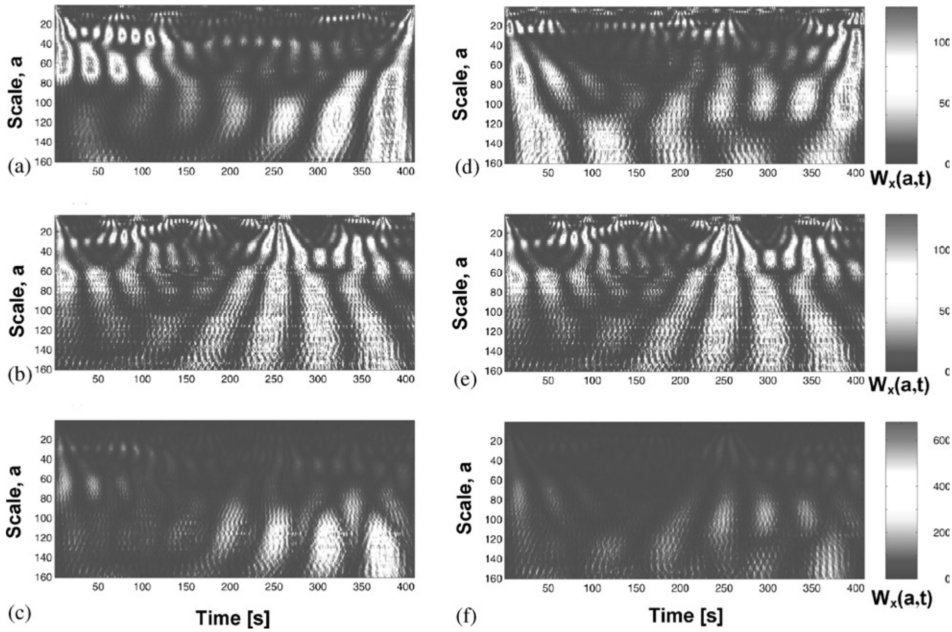

Fig. 4. (a) Scalogram of upstream wind velocity 1; (b) scalogram of rooftop pressure; (c) coscalogram of these two correlated processes; (d) scalogram of upstream wind velocity 2; (e) scalogram of rooftop pressure; (f) coscalogram of these two uncorrelated processes (after [8]).

uncorrelated, for which no marked white pockets, indicative of correlation, are present.

This coscalogram contains wavelet coefficients determined from segments of the signal isolated by the sliding window of the scaled parent wavelet. At each time step, these wavelet coefficients can be imagined to comprise a single raw spectrum across the range of scales, equivalent to a spectrum obtained from a single block of time history in the traditional Fourier analysis. These raw spectra ordered sequentially along the time axis in the scalogram and coscalogram lack the ensemble averaging necessary in traditional Fourier methods to reduce the variance in the estimate, resulting in noisy displays where correlated events are difficult to differentiate from random coincident coefficients. This explains the presence of the subtle light pockets, indicative of spurious correlation, present in both the correlated and uncorrelated examples in Fig. 4.

2.4. *Wavelet-based coherence and bicoherence*

Though this simple measure of correlation has been used to qualitatively identify first-order wind velocity and pressure relationships [8], it is refined in [9] by the introduction of a wavelet coherence measure used to produce a time-frequency display of the coherence between signals intermittently correlated. The traditional form of the coherence function can be retained as the ratio of the wavelet cross-spectrum to the product of the wavelet auto-spectra of the two signals $x(t)$ and $y(t)$. The wavelet coherence map is thus defined as

$$(c^W(a,t))^2 = \frac{|S^W_{xy}(a,t)|^2}{S^W_{xx}(a,t)S^W_{yy}(a,t)}, \tag{6}$$

where the localized power spectra discussed above are given by

$$S^W_{ij}(a,t) = \int_T W_i^*(a,t)\, W_j(a,t)\, \mathrm{d}\tau. \tag{7}$$

The localized time integration window in Eq. (7), $T = [t - \Delta T, t + \Delta T]$, is selected based on the time resolution desired in the resulting coherence map and essentially performs the same ensemble averaging operation, albeit localized in time, as traditional Fourier analysis to obtain an auto-spectrum or cross-spectrum of two signals.

As evident in Fig. 4, an insufficient amount of ensemble averaging can lead to considerable statistical noise and produce spurious correlations. Thus, a framework was developed to identify the source of statistical noise in the raw wavelet coscalograms and propose a variety of remedies [9]. The initial introduction of a variable integration window, predicated on the multi-resolution character of wavelets, verified that the lack of ensemble averaging results in much of the observed spurious coherence, though the application of this remedy is constrained by the ensuing loss in temporal resolution. The theory of ridges is briefly introduced in [9] alongside the concept of hard thresholding to generate a coarse ridge extraction scheme to isolate meaningful coherence. This technique, when coupled with sufficient ensembles in the aforementioned variable integration scheme, is shown to enhance performance. However, to preserve evolutionary characteristics while removing significant noise, more sophisticated approaches are required, which do not involve extensive averaging. As a result, a "smart" thresholding simulation scheme is proposed to provide a reference noise map to separate spurious noise effects from true signal content. In this approach, the noise is filtered from the wavelet coherence map by comparison with a threshold describing the likely noise level. This threshold is created by averaging a series of reference correlation maps between one signal and uncorrelated simulations of the second signal, which match the second signal's spectral and probabilistic characteristics. As shown in Fig. 5, which displays the wavelet coherence for measured wind velocity and pressure on a full-scale building, by specifying the desired probability of noise exceeding the threshold level, in essence regulating the extent of filtering, the spurious coherence is progressively removed from the map. What remains in Fig. 5f is the true coherence between wind velocity and pressure for this measured data.

The analysis developed for first-order correlation detection is further extended to higher-order correlation [9], as some of the processes under investigation may not be linearly related, e.g., wind velocity fluctuations and associated pressure fluctuations. Furthermore, intermittent bursts of strong second-order correlation cannot be identified by applying a Fourier-based analysis over short-time intervals without the

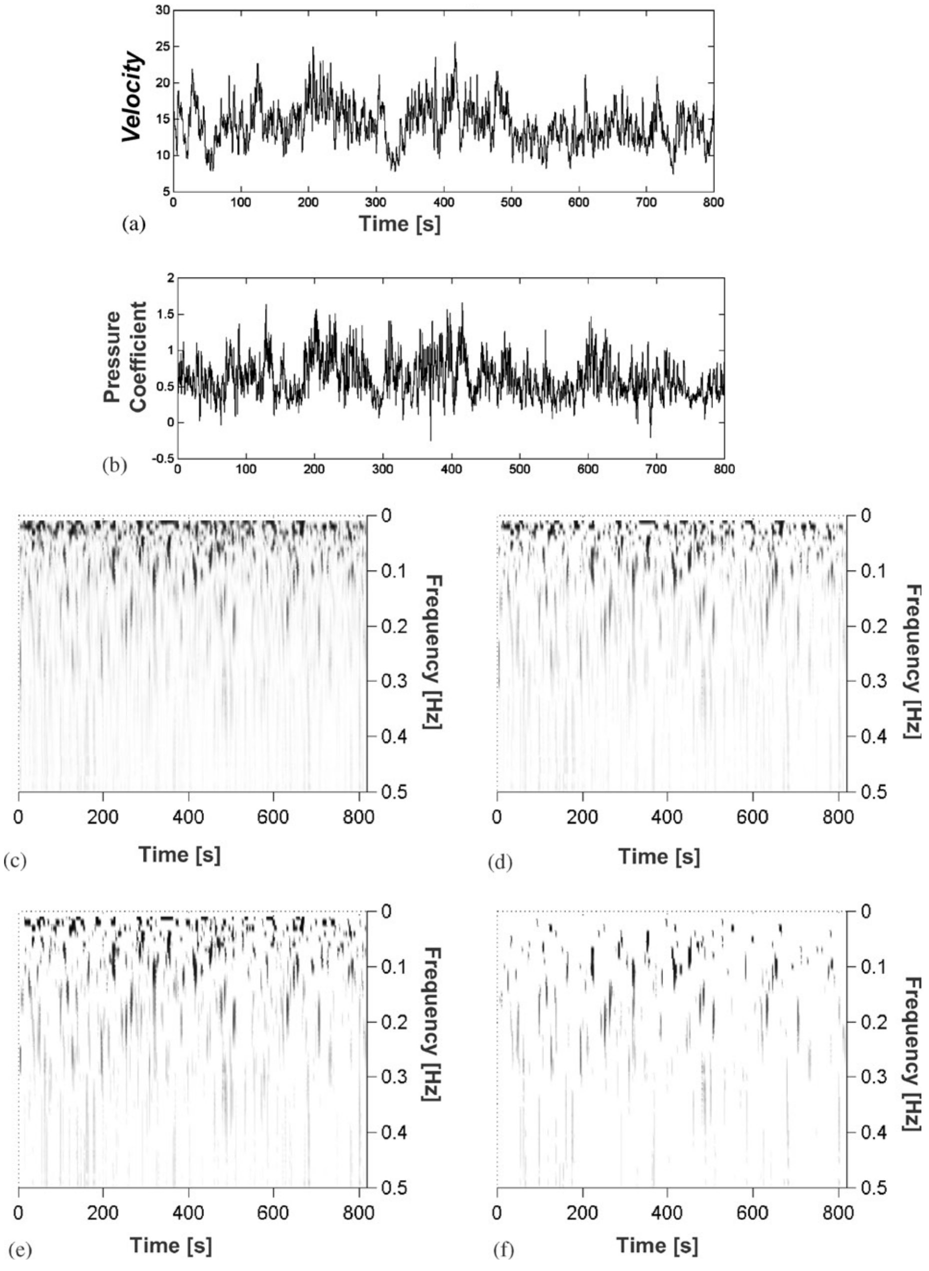

Fig. 5. (a) Measured wind velocity; (b) measured wind pressure; (c) unfiltered wavelet coherence map; filtered wavelet coherence map for varying levels of noise exceedence: (d) 25% exceedence; (e) 10% exceedence; (f) 1% exceedence (after [9]).

benefit of additional variance reduction schemes. In this context, bicoherence, the ratio of the higher-order cross-bispectrum to the first-order spectra, is utilized as a metric for assessing the presence of second-order correlation (e.g. [12–13]). The bicoherence is defined as

$$B^W_{xxy}(a_1, a_2, t) = \int_T W_x(a_1, \tau) W_x(a_2, \tau) W_y(a, \tau)\, \mathrm{d}\tau, \tag{8}$$

where

$$\frac{1}{a} = \frac{1}{a_1} + \frac{1}{a_2} \tag{9}$$

is used in the evaluation of the wavelet bicoherence:

$$(b^W_{xxy}(a_1, a_2, t))^2 = \frac{|B^W_{xxy}(a_1, a_2, t)|^2}{\int_T |W_x(a_1, \tau)\ W_x(a_2, \tau)|^2\, \mathrm{d}\tau \int_T |W_y(a, \tau)|^2\, \mathrm{d}\tau}. \tag{10}$$

The extension of the wavelet-based spectral estimation of coherence and the aforementioned statistical noise remedies permit the development of a filtered wavelet bicoherence map [9], as shown in Fig. 6, where the wind velocity and pressure being analyzed are second-order correlated over only selected frequencies and over selected time intervals. By again defining the desired level of exceedence, the spurious higher-order coherence is removed in the last two plots of the figure. Note that specification of a more stringent exceedence criteria would remove any residual spikes shown in those last two plots.

These two demonstrations and other examples in [9] affirm that this wavelet-based technique is capable of identifying both first- and second-order correlation and effectively reducing the presence of noise for both simulated and measured data. Its robustness is further established as it is shown to alleviate the presence of spurious coherence, even in cases where variance and leakage are prevalent. Though relatively

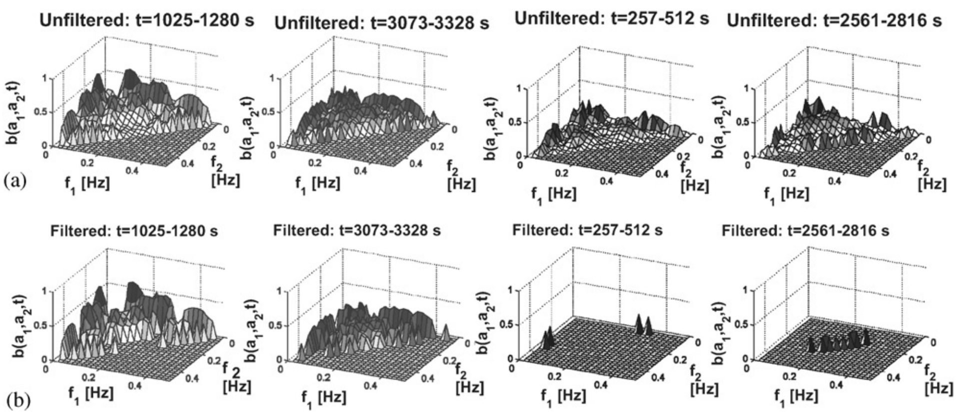

Fig. 6. Wavelet bicoherence maps between wind velocity and pressure: (a) unfiltered; (b) filtered. Signals are correlated over 1025–1280 and 3073–3328 s, uncorrelated over 257–512 and 2561–2816 s (after [9]).

intensive, this approach facilitates the removal of significant levels of all of the various contributing noise sources.

2.5. Time domain applications: wavelet transforms for system identification

The time-frequency character of wavelet transforms allows increased flexibility—as both traditional time and frequency domain system identification approaches can be exploited to examine nonlinear and nonstationary features that are in essence obscured by traditional spectral approaches, as they provide an averaged-sense of the system's response quantities. From the perspective of Civil Engineering applications, there is considerable need to escape from the realm of averaged quantities, since there is direct interest in correlating measured dynamic properties of natural frequency and damping to specific levels of response amplitude. However, to establish the nonlinear characteristics of a dynamic parameter such as damping, whose complex mechanisms and properties have proven difficult to accurately quantify, engineers must be equipped with sophisticated mathematical tools that will permit them to accurately track the variations in dynamic properties over the course of varying ambient loadings. Without reliable estimations of such behavior, satisfactory performance of structures cannot be insured and the state-of-the-art in structural design cannot advance.

To address this pressing issue, an analysis framework is proposed, predicated on the Morlet wavelet introduced previously, which can overcome the limitations of stationarity and permit tracking of amplitude-dependent dynamic features. Such tracking of time-varying frequency content is typically accomplished by monitoring the IF of the signal. Although there have been contributions from a number of researchers, the common definition of this quantity is traced back to the notion of a complex analytical signal [4], taking the form of an exponential function given by

$$z(t) = A(t)e^{i\phi(t)} \tag{11}$$

with time-varying amplitude $A(t)$ and phase $\phi(t)$. Typically, this complex analytic signal is generated by

$$z(t) = x(t) + i\,H[x(t)], \tag{12}$$

where $x(t)$ is the real-valued signal being transformed and the operator $H[\cdot]$ represents the Hilbert Transform. Since the Hilbert Transform essentially performs a 90° phase shift, $x(t)$ and $H[x(t)]$ are said to be in quadrature.

From the definition in Eq. (11), Ville [14] proposed the concept of IF as the time-varying derivative of the phase

$$f_i(t) = \frac{1}{2\pi}\frac{d}{dt}\phi(t) = \frac{1}{2\pi}\frac{d}{dt}[\angle z(t)] \tag{13}$$

providing a simple means to identify the time-varying frequency of a signal. Though this is a widely accepted approach, the Hilbert Transform in Eq. (12) can only be applied to single-degree-of-freedom (SDOF) responses or monocomponent signals. Thus, a form of bandpass filtering is often required as a precursor to the Hilbert

Transform operation in Eq. (12). The wavelet provides a convenient way to overcome this limitation.

As discussed previously in the context of Fig. 3, the ridge is defined by the scales at which the signal takes on its maximum value. More importantly, the real and imaginary wavelet coefficient-pairs along the ridge (skeleton) are respectively proportional to the signal and its quadrature components [15]. As discussed in [10,15], these complex coefficients can be used directly in a traditional system identification approach based on the analytic signal theory discussed above. For multi-degree-of-freedom signals, the wavelet scalogram will manifest multiple ridges. By examining the phase of the wavelet skeletons for each respective ridge the time-varying IF can be identified.

Specifically, in the case of free vibration decay curves, in each mode the oscillator responds at the damped natural frequency ω_D, and the time-varying amplitude term takes the form of an exponential, decaying based on the system's natural frequency $\omega_n = 2\pi f_n$ and damping $\xi(\omega_D \sim \omega_n$, for lightly damped systems) in that mode, according to

$$z(t) = (A_0 e^{-\xi\omega_n t})e^{i(\omega_D t+\theta)}, \tag{14}$$

where A_0 is an initial amplitude value and θ is a phase shift. Thus, the derivative of the wavelet phase of each skeleton provides a natural frequency estimate for a given mode, which can then be used to determine the damping from the slope of the natural log of the amplitude term, according to Eq. (14).

Even in situations where free vibration decays are not directly available, this wavelet-based system identification approach may still be implemented. As shown in the example in Fig. 7, the Random Decrement Technique [16–17] is used to preprocess the response of a structure under random excitation, in this case the acceleration of a full-scale tower under typhoon winds, yielding a Random Decrement Signature (RDS) proportional to the free vibration response of the structure. The signature in its current form contains the contributions of multiple modes and measurement noise and is not the smooth stable decay one would expect from an SDOF oscillator. However, processing this through the CWT permits the dominant mode to be readily identified and isolated. The wavelet skeleton associated with this mode yields the anticipated decay associated with an SDOF oscillator. Note that both the wavelet scalogram and skeleton are complex-valued, though only the real component is shown in Fig. 7 for simplicity. This slope of the skeleton's phase and amplitude may be analyzed to determine the natural frequency and damping, respectively, as discussed previously. As shown in [10], the frequency was estimated at 0.645 Hz and critical damping ratio at 0.0151, though showing some slight variations. These findings were consistent with those observed in free vibration testing [18].

2.6. Frequency domain applications: instantaneous power spectra and damping

Though the previous approach was largely rooted in the time domain, frequency domain perspectives from the wavelet coefficients are also insightful. To

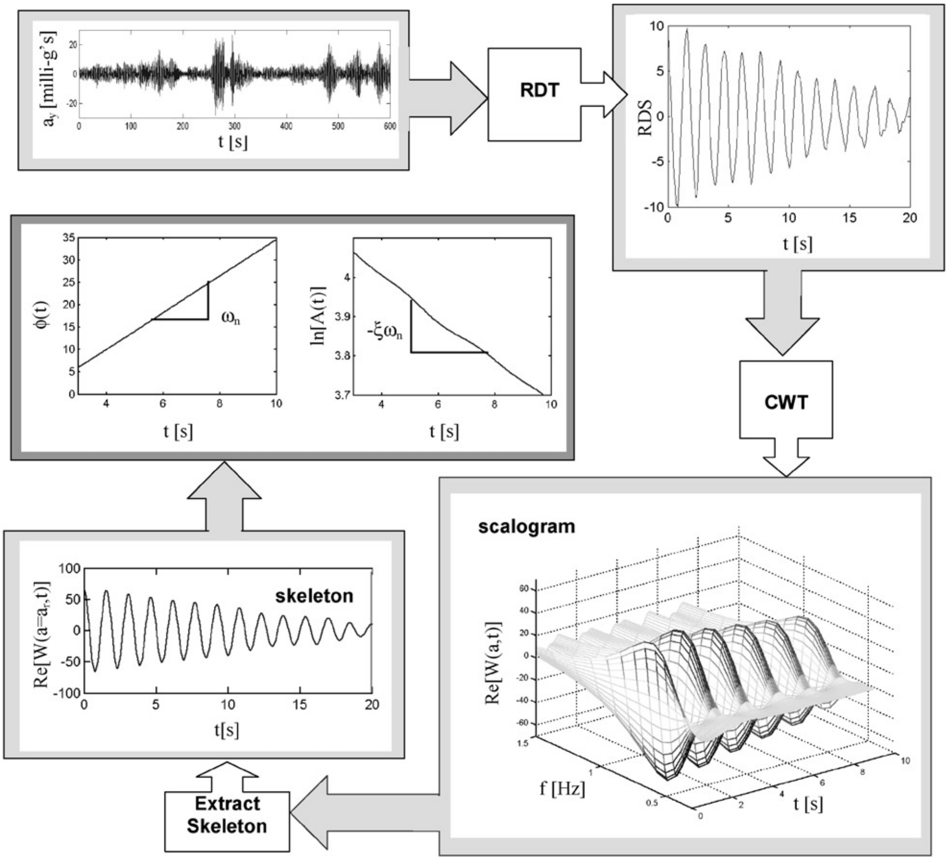

Fig. 7. Flow chart explaining wavelet-based system identification in time domain.

demonstrate, the scalogram of the sinusoidal chirp discussed previously in Fig. 3, is shown again in Fig. 8. However, in this case, at a given time, the values of the wavelet coefficients across the range of frequencies are extracted to produce an instantaneous power spectrum, focused at the IF of the signal.

To illustrate how this approach can be used in the analysis of measured signals, consider the output of one experimental measuring station as wind-generated random sea waves are physically simulated by a JONSAWP random excitation in Fig. 9a. The scalogram in Fig. 9b reflects several pockets of intense energy bursts, associated with high amplitude events in the data, and concentrated at around 0.5 Hz. The presence of white pockets fading into the high frequency range suggests the detection of a distribution of energy beyond the fundamental observed frequency. Ridge extraction from the wavelet modulus revealed up to three local maxima for any given instantaneous spectrum. The maxima take on the highest values in the vicinity of 0.5 Hz, accompanied by intermittent lower amplitude components at relatively lower and higher frequencies. Individual analyses of the

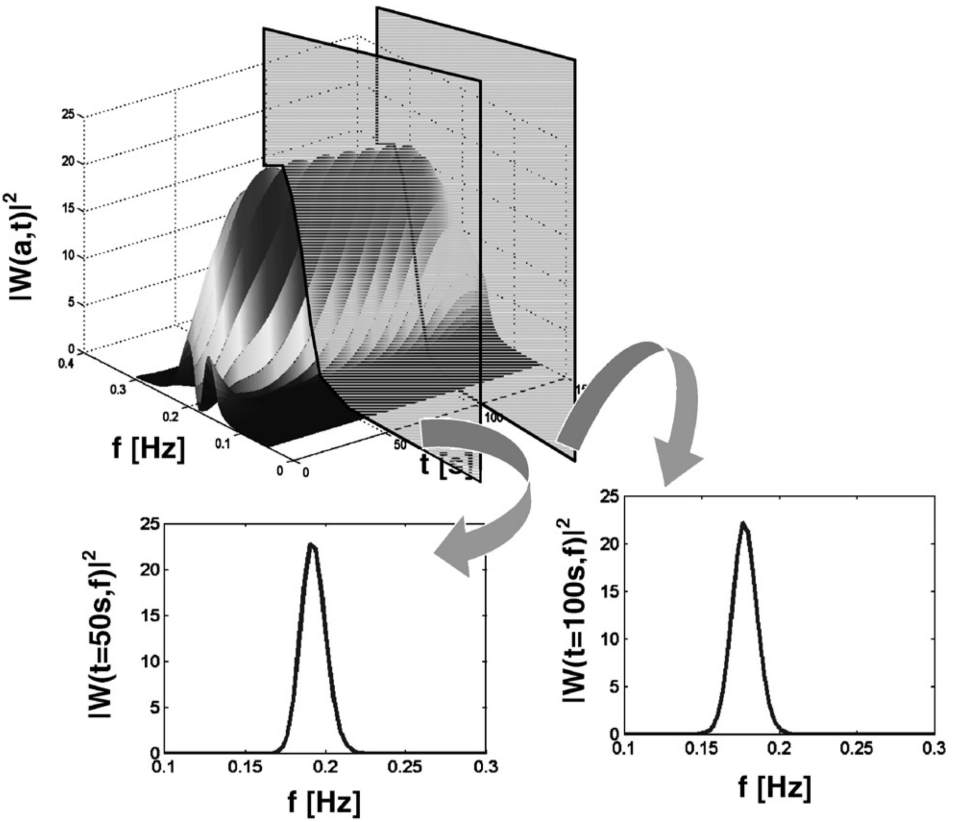

Fig. 8. Wavelet scalogram and instantaneous power spectra.

occurrence of the three ridges are provided in Fig. 9c–e. Fig. 9c displays the IF associated with the simplest harmonic representation observed in the signal—for which there is only one dominant oscillatory component near 0.5 Hz, typified by the instantaneous spectrum to the right. The frequency content of the signal often shifts then to a bi-modal characteristic, centered around 0.5 Hz, as shown in Fig. 9d, but alternating its dominant peak between approximately 0.4 and 0.6 Hz, as shown by the two example instantaneous spectra. The occurrence of a third peak in Fig. 9e is usually an intermittent phenomenon of relatively lower energy and accompanies the dominant presence of the same two harmonics centered near 0.5 Hz. It is important to reiterate that wavelet IF estimates, when viewed in tandem with the wavelet IF spectra, serve as a microscope for studying the evolution of multiple harmonic components within the response. In particular, the alternating characteristic of the two dominant components centered near 0.5 Hz represents a temporal variation of the fundamental wave frequency that would be obscured in traditional Fourier analysis.

However, the frequency at which the instantaneous spectra concentrate is not the only useful information. The spectra also have measurable spread about this

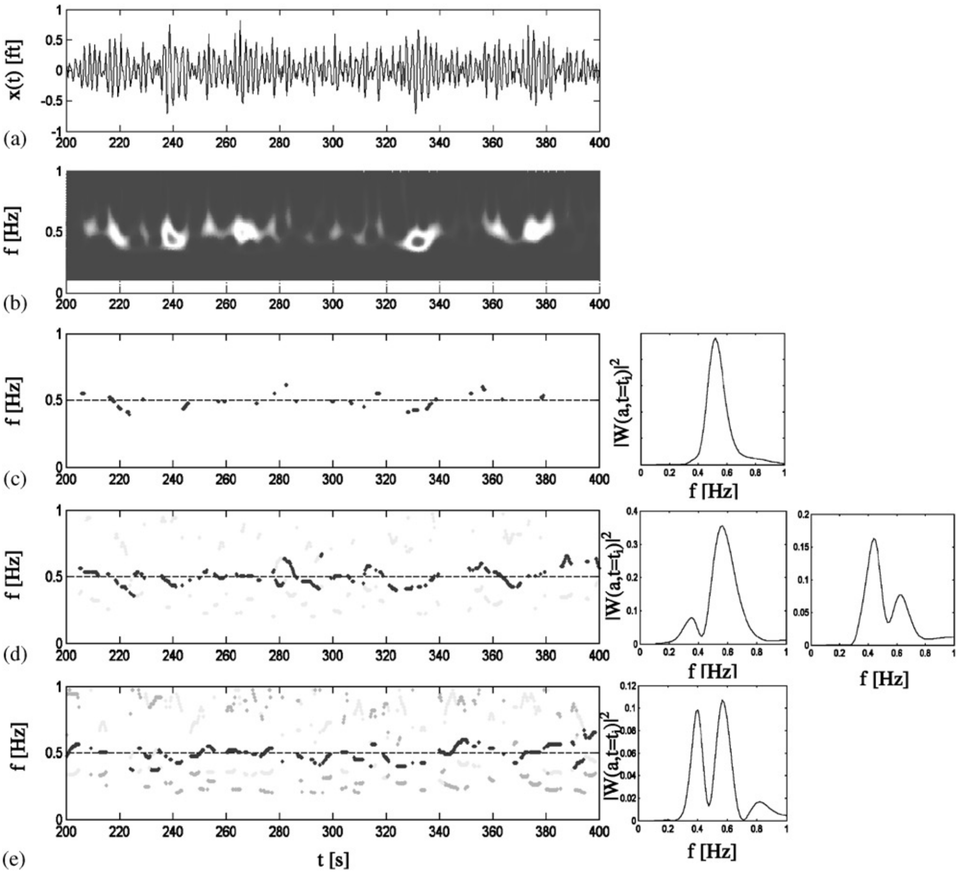

Fig. 9. (a) Measured wind-generated random wave data; (b) wavelet scalogram; IF identified from (c) single mode ridge; (d) bi-modal ridge; (e) multi-mode ridge (dark lines indicate highest energy component at that time step), with example of each instantaneous spectra class shown at the right.

frequency indicative of the instantaneous bandwidth of the signal. Wavelets essentially fit small waves or so-called "wavelets" to the signal at each point in time. In the case of the Morlet wavelet, these localized waves are sinusoidal in nature. The IF identified by the peak in the spectra of Fig. 8 corresponds to the frequency of the sinusoid that is a best-fit at that instant in time. However, if the wave profile subtlety deviates from a simple sinusoid, it is not unreasonable to expect that additional neighboring frequencies are required to capture these deviations. Thus, at an instant in time, a wavelet instantaneous spectrum peaks at the IF or the dominant frequency, but also manifests measurable spread indicating that other frequency components are present to a lesser extent at that instant in time. The involvement of such adjacent frequencies is represented by the bandwidth measure. Thus, in the truest sense, the wavelet IF is the mean frequency and the bandwidth reflects the deviation of these frequencies from this mean as they evolve in time [19].

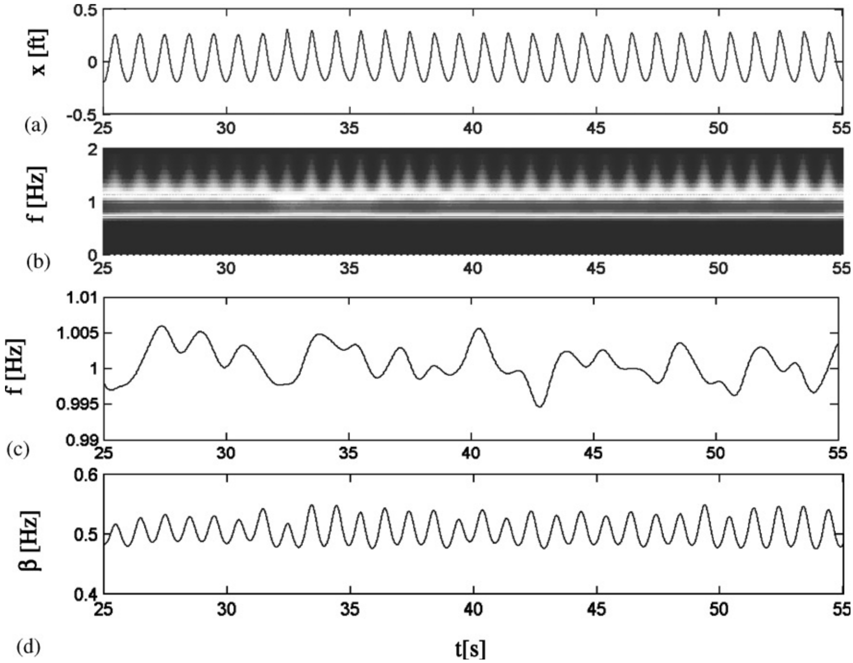

Fig. 10. (a) Thirty seconds of wind-generated wave surface elevation; (b) scalogram of wave data; (c) IF from wavelet phase; (d) instantaneous bandwidth estimate.

While the evolution of IF and bandwidth for a number of nonstationary and nonlinear systems is studied in more detail in [9], one example is provided here for illustration. In Fig. 10, the surface elevation of wind-generated waves mechanically simulated in a wave tank is measured. The measured data is provided in Fig. 10a and manifests narrowed peaks and widened toughs, highlighting a subtle deviation from a simple sinusoidal shape. The scalogram in Fig. 10b concentrates near 1 Hz shown by a dark band enveloped in white, but the periodic excursion of energy into the higher frequency scales indicates the presence of time-varying frequency content. From the phase-based IF estimate, in Fig. 10c, the minor modulations reveal time-variance in the local mean frequency. Further fluctuations about this mean frequency are then identified in the instantaneous bandwidth in Fig. 10d, which provides a rich display of nonlinear characteristics. The periodic modulations of the bandwidth indicate a regular variation of frequencies concomitant at each instant in the signal.

3. Conclusions

Just as the Fourier transform has introduced spectral analysis to the practicing engineer, current efforts are focused on ushering in a new analysis framework in the time-frequency domain, bringing innovative mathematical tools such as wavelet transforms to practicing engineers, permitting accurate analysis without the restrictions of stationarity. The extension of wavelet transforms to the estimation of time-varying energy density permits the tracking of evolutionary characteristics in the signal and the development of measures like wavelet-based coherence to capture intermittent correlated structures in signals. Further, the wavelet's dual nature, being a simultaneous transform in the time and frequency domains, can be exploited to permit the adaptation of a number of traditional system identification and analysis schemes. Despite the merits of these analyses, it should be noted that a number of processing concerns must be addressed in order to obtain reasonable results, particularly for the class of signals of relevance to Civil Engineering [9–11]. Though the application of wavelet transforms in Civil Engineering is in its infancy, its future shows great promise as a tool to redefine the probabilistic and statistical analysis of wind effects.

Acknowledgements

The authors gratefully acknowledge support from NSF Grant CMS 00-85109, the NASA Indiana Space Grant, and the Center for Applied Mathematics at the University of Notre Dame. The authors are also appreciative of the intellectual contributions of Dr. Kurtis Gurley of the University of Florida at Gainesville.

References

[1] A. Kareem, Wind effects on structures: a probabilistic viewpoint, Prob. Eng. Mech. 2 (4) (1987) 166–200.
[2] A. Kareem, Analysis and modeling of wind effects: numerical techniques, in: A. Larsen, G.L. Larose, F.M. Livesey (Eds.), Wind Engineering into the 21st Century, Balkema Press, Rotterdam, pp. 43–54.
[3] A. Kareem, Modeling and simulation of wind effects: a reflection on the past and outlook for the future, in: C.-K. Choi, G. Solari, J. Kanda, A. Kareem (Eds.), First International Symposium on Wind and Structures for the 21st Century, Techno Press, Seoul, 2000.
[4] D. Gabor, Theory of communication, Proc. IEEE 93 (III) (1946) 429–457.
[5] R.A. Carmona, W.L. Hwang, B. Torresani, Wavelet Analysis and Applications: Practical Time-Frequency Analysis, Vol. 9, Academic Press, San Diego, 1998.
[6] S. Mallat, A Wavelet Tour of Signal Processing, Academic Press, San Diego, 1998.
[7] A. Grossman, J. Morlet, Decompositions of functions into wavelets of constant shape and related transforms, in: L. Streit (Ed.), Mathematics and Physics, Lecture on Recent Results, World Scientific, Singapore, 1985, pp. 135–165.
[8] K. Gurley, A. Kareem, Applications of wavelet transforms in earthquake, wind and ocean engineering, Eng. Struct. 21 (1999) 149–167.
[9] K. Gurley, T. Kijewski, A. Kareem, First and higher-order correlation detection using wavelet transforms, J. Eng. Mech. ASCE (2002), in press.
[10] T. Kijewski, A. Kareem, Wavelet transforms for system identification in civil engineering, Comput.-Aided Civil Infrastruct. Eng. (2002), in press.
[11] T. Kijewski, A. Kareem, 2002. Time-frequency analysis: revisiting the efficacy of Hilbert spectra and wavelet transforms, Proc. Roy. Soc. A, submitted for publication.
[12] C.L. Nikias, A.P. Petropulu, Higher-Order Spectral Analysis, a Nonlinear Signal Processing Framework, PTR Prentice-Hall, New Jersey, 1993.

[13] K. Gurley, M. Tognarelli, A. Kareem, Analysis and simulation tools for wind engineering, Prob. Eng. Mech. 12 (1) (1997) 9–31.
[14] J. Ville, Theorie et Application de la Notion de Signal Analytical, Cables Trans. 2A (1) (1948) 61–74.
[15] W.J. Staszewski, Identification of damping in MDOF systems using time-scale decomposition, J. Sound Vib. 203 (2) (1997) 283–305.
[16] H.A. Cole, On-line Failure Detection and Damping Measurement of Aerospace Structures by Random Decrement Signatures, NASA CR-2205, 1973.
[17] K. Gurley, A. Kareem, Damping in structures: its evaluation and treatment of uncertainty, J. Wind Eng. Ind. Aerodyn. 59 (2,3) (1996) 131–157.
[18] Y. Tamura, K. Shimada, H. Kazuki, Wind response of a tower (Typhoon Observation at the Nagasaki Huis Ten Bosch Domtoren), J. Wind Eng. Ind. Aerodyn. 50 (1993) 309–318.
[19] M.B. Priestley, Non-linear and Non-stationary Time-series Analysis, 1st Edition, Academic Press, San Diego, 1988, pp. 140–174 (Chapter 6).